Developmental Biology **217,** 375–385 (2000)
doi:10.1006/dbio.1999.9542, available online at http://www.idealibrary.com on IDEAL®

Presence and Roles of Calcium Gradients along the Dorsal-Ventral Axis in Drosophila Embryos

Robbert Créton,[1] Jill A. Kreiling, and Lionel F. Jaffe
Marine Biological Laboratory, Woods Hole, Massachusetts 02543

Dorsal-ventral specification of the Drosophila embryo is mediated by signaling pathways which have been very well described in genetic terms. However, little is known about the physiology of Drosophila development. By imaging patterns of free cytosolic calcium in Drosophila embryos, we found that several calcium gradients are generated along the dorsal-ventral axis. The most pronounced gradient is formed during stage 5, in which calcium levels are high dorsally. Manipulation of the stage 5 calcium gradient affects specification of the amnioserosa, the dorsal-most region of the embryo. We further show that this calcium gradient is inhibited in *pipe, Toll,* and *dorsal* mutants, but is unaltered in *decapentaplegic (dpp)* or *punt* mutants, suggesting that the stage 5 calcium gradient is formed by a suppression of ventral calcium concentrations. We conclude that calcium plays a role in specification of the dorsal embryonic region.

Key Words: **pattern formation; embryonic development; signaling pathways; dorsoventral axis; [Ca^{2+}]; TGF-β; aequorin; imaging photon detector.**

INTRODUCTION

The establishment of pattern along the dorsal-ventral axis of Drosophila embryos involves the activation of two separate pathways within the thin, perivitelline space between the plasma and the vitelline membranes. First, the *spatzle-Toll* pathway is activated ventrally and then the *decapentaplegic (dpp)* pathway is activated dorsally (Morisato and Anderson, 1995; Anderson, 1998).

The spatial coordinates of the *spatzle-Toll* signaling pathway are set up during oogenesis (Sen *et al.,* 1998). However, the activation of this pathway occurs after fertilization. First, a protease cascade is activated in the ventral extracellular region, which leads to the proteolytic activation of the ligand Spatzle (reviewed by Anderson, 1998). Processed Spatzle activates the plasma membrane receptor Toll, and Toll initiates a cytoplasmic signaling pathway involving the proteins Tube, Pelle, Cactus, and Dorsal (Dl) (reviewed by Belvin and Anderson, 1996). As a final step in the cytoplasmic signaling pathway, Dl forms a nuclear concentration gradient along the dorsal-ventral axis, with the highest Dl concentrations in the ventral nuclei (Roth *et al.,* 1989; Rushlow *et al.,* 1989; Steward, 1989). The nuclear localization of Dl plays a central role in the regulation of gene expression along the dorsal-ventral axis of the embryo. Dl activates the expression of *twist* and *snail* and inhibits the expression of *dpp, zerknullt (zen),* and *tolloid (tld)* (reviewed by Morisato and Anderson, 1995).

The *dpp* pathway is activated in the dorsal region of the embryo and starts with the transcription, translation, and secretion of Dpp (Padgett *et al.,* 1987; Ferguson and Anderson, 1992a). Dpp forms an extracellular activity gradient (Wharton *et al.,* 1993) by interacting with other extracellular proteins such as Sog and Tld (Ferguson and Anderson, 1992b; Marques *et al.,* 1997; Mullins, 1998; Ashe and Levine, 1999). Activated Dpp binds to a complex of plasma membrane receptors consisting of type I (sax and tkv) and type II (punt) receptors (reviewed by Ten Dijke *et al.,* 1996; Massague, 1998). These receptors are serine-threonine kinases which phosphorylate the Mad protein, which is a cytoplasmic messenger of the Smad family. Mad may bind to other Smad proteins, such as Medea, and translocates into the nucleus to control specification of the dorsal region (reviewed by Raftery and Sutherland, 1999). Similar mechanisms are believed to operate in vertebrate development. Dpp is a member of the TFG-beta superfamiy and shows strong homology with the vertebrate bone morphogenetic proteins BMP-2 and BMP-4 (Padgett *et al.,* 1987; Wall and Hogan, 1994; Massagué *et al.,* 1994). Moreover, both the Dpp receptors and the cytoplasmic signaling proteins Mad and Medea have homologous counterparts in vertebrates (Raftery and Sutherland, 1999). The BMP's play a role in

[1] Present address: Brown University School of Medicine, Department of Obstetrics and Gynecology, Women and Infants Hospital, 101 Dudley Street, Providence, RI 02905.

0012-1606/00 $35.00

specification of pattern along the dorsal-ventral axis in Xenopus and zebrafish embryos, although the axis seems to be reversed (reviewed by Ferguson 1996; Holley and Ferguson 1997; Mullins, 1998).

Thus, the nature, order of action, and loci of most of the participating proteins have been determined. In contrast, the physiology of Drosophila development is still a relatively unexplored field. In particular, little is known about calcium signaling in early Drosophila development (reviewed by Beckingham, 1995). Most of what is known points to a role of calcium in specification of the ventral embryonic region. A role of calcium in ventral specification was predicted long ago (Jaffe, 1986) and two recent lines of evidence support this idea. The first line of evidence comes from studies in cell lines. It was shown that an elevation of calcium induces a rapid destruction of the anchor protein Cactus and induces the translocation of Dl into the nucleus (Kubota *et al.,* 1993; Kubota and Gay, 1995). The second line of evidence is the analysis of maternal effects in calmodulin mutants (Nelson *et al.,* 1997). Defects in embryonic dorsal-ventral patterning were observed and were reported to be associated with reduced levels of nuclear Dl protein. Thus both lines of evidence suggest that calcium may act as one of the steps in the signaling pathway between Toll activation in the plasma membrane and Dl translocation in the nucleus. However, beyond this, the roles of calcium in dorsal-ventral patterning remain unclear. In particular, nothing is known of the roles of calcium in the second, dorsally active *dpp* pathway.

In this report we describe the presence of steady calcium gradients during the first 6 h of embryonic development using the chemiluminescent aequorins as calcium reporters. This is the first description of calcium patterns in Drosophila development. A striking calcium gradient was found during stage 5. This gradient was shown to play a role in specification of the dorsal embryonic region.

MATERIAL AND METHODS

Calcium imaging with chemiluminescence. Freshly laid eggs of wild type flies (Oregon R) were dechorionated on double stick tape, glued onto a coverslip, dried for 5 min, and covered with halocarbon oil (Sigma No. 27 and No. 700 mixed 1:2). The embryos were kept at room temperature (23°C) at all times. The embryos were microinjected at the posterior pole with the chemiluminescent calcium indicator *h*-aequorin, which was kindly provided by Dr. O. Shimomura. We injected 0.1 nl of a 0.5 mM *h*-aequorin solution. Luminescence was imaged with an imaging photon detector (IPD), which is mounted on a Zeiss Axiovert microscope. We used a 40× oil objective (Zeiss plan-neofluar), which has a high NA (1.30) and provides good spatial resolution. The output was stored digitally as a list of photon events, allowing luminescence to be quantified at specific locations and during various periods of time. Every 10 min the recording was interrupted for a few seconds to take a bright-field video image of the embryo. These video images were used to determine the exact developmental stage of the imaged embryo (see Wieschaus and Nusslein-Volhard, 1986). The time of oviposition (T_0) was calculated by subtracting 80 min from the onset of pole cell formation. Methods of aequorin injection and photon imaging have been described in detail by Créton *et al.* (1999).

Calibration of luminescence. Luminescence was calibrated in order to calculate the corresponding calcium concentrations. To this end, embryos were injected with *h*-aequorin plus 0.1 nl of a calcium buffer containing 250 mM tetrapotassium-BAPTA, 81 mM $CaCl_2$, and 10 mM Tris 7.5, which clamps the cytosolic free calcium concentration at 100 nM. The luminescence of these embryos averaged 4.2 milliphotons/pixel second (n = 11, SE = 0.2). To calculate other calcium concentrations we assumed that luminescence is proportional with the 2.1 power of the calcium concentration (Shimomura and Inouye, 1996). Using these values, we formulated the following equation: $L = 2.1 \times 10^{15}\ (Ca^{2+})^{2.1}$, with the luminescence, L, in milliphotons per pixel second (mp/ps) and $[Ca^{2+}]$ in moles/liter.

Ratiometric calcium imaging with confocal microscopy. Embryos were microinjected posteriorly with 0.1 nl of a dye mixture, containing 5 mM calcium green–1 dextran, MW = 10.000 (contains an average of 1.1 calcium green molecules per dextran molecule), and 10 mM Texas red dextran, MW = 10.000 (Molecular Probes). Fluorescence was imaged in late stage 5 embryos on a Zeiss LSM 510 confocal microscope using a 488-nm laser for excitation. Emitted light was recorded using a 505–550 nm band-pass filter for calcium green dextran and a 585-nm long-pass filter for Texas red dextran. The calcium green/Texas red ratio was color-coded in a spectrum from blue to red (ratio of 1.0–1.1), in which red represents the highest calcium concentrations.

Manipulation of calcium patterns with BAPTA buffers. Embryos were injected posteriorly with 0.1 nl of the following buffers to manipulate the endogenous calcium patterns of the embryo: (a) 25 mM dibromo-$BAPTA_{50}$, containing 25 mM dibromo-BAPTA, 0.8 mM $CaCl_2$, and 2 mM Tris 7.5, setting the free calcium concentration at 50 nM; (b) 50 mM dibromo-$BAPTA_{50}$, containing 50 mM dibromo-BAPTA, 1.6 mM $CaCl_2$, and 2 mM Tris 7.5, setting the free calcium concentration at 50 nM; (c) 100 mM dibromo-$BAPTA_{50}$, containing 100 mM dibromo-BAPTA, 3.2 mM $CaCl_2$, and 2 mM Tris 7.5, setting the free calcium concentration at 50 nM; (d) 100 mM dibromo-$BAPTA_{2000}$, containing 100 mM dibromo-BAPTA, 57 mM $CaCl_2$, and 2 mM Tris 7.5, setting the free calcium concentration at 2000 nM; and (e) 100 mM K_4-$BAPTA_{50}$, containing 100 mM BAPTA, 19 mM $CaCl_2$, and 2 mM Tris 7.5, setting the free calcium concentration at 50 nM. The BAPTAs were obtained from Molecular Probes as tetrapotassium salts (K_4-BAPTA thus refers to the "regular" BAPTA). The concentrations of free cytosolic calcium are indicated by the lowercase numbers (in nM). The equations for calculating free calcium concentrations have been described by Créton *et al.* (1999).

Determination of final cytosolic concentrations. We estimated the final cytosolic concentrations of injected BAPTA calcium buffers (and of injected aequorin) to be 3% of the concentration in the injectates for these reasons: First we divided the 0.1-nl volume of injectate by the 10-nl volume of the egg to yield 1%. Then we tripled this by somewhat arbitrarily assuming that two-thirds of the preblastoderm cytoplasm consists of components—particularly yolk, lipid, mitochondria, and ER–that should be inaccessible to the highly hydrophilic and biologically inert aequorin reporter and BAPTA buffers.

Kr-lacZ expression. A Drosophila line was used in which the *lacZ* gene is driven by a *Kruppel* promoter (the *Kr-lacZ* line was kindly provided by Dr. Konrad Basler). These embryos express β-galactosidase in the amnioserosa (see, e.g., Ferguson and Ander-

son, 1992a), which can be detected by a simple three-step method. Dechorionated stage 14 embryos were permeabilized in heptane for 5 min, fixed in 4% formaldehyde in PBS for 5 min, and stained overnight in an X-gal solution, containing 2% X-gal (diluted from a 20× stock in dimethylformamide), 100 mM K_3FeCN, 100 mM K_4FeCN, 1% Triton, in PBS, pH 7.3. Photographs were made on a Zeiss microscope using a combination of transmitted light and a dark field ring.

Mutant analysis. Calcium was imaged in the mutants *pipe, Toll*^{10B}, *dl, Dpp,* and *punt*. The first three lines have mutations in a maternal gene, the latter two in a zygotic gene. The [pipe^{664} st e/DTS4 th st e Sb] line was kindly provided by Dr. Carl Hashimoto. All embryos from *pipe*^{664}/*pipe*^{664} are dorsalized. The [Tl^{10B} e/OR60/TM3 Sb e] line was also provided by Dr. Carl Hashimoto. All embryos from *Tl*^{10B}/+ are ventralized. The [dl^1 cn^1 sca^1/CyO DTS100] line was obtained from the Bloomington stock center. All embryos from *dl*^{1}/*dl*^{1} are dorsalized. The [dpp^{H46} wg^1 cn^1 bw^1/CyO-P23, P{dpp [+ t20] ry [t7.2] = dpp − Sal20}2 − 1]] line was obtained from the Bloomington stock center; 25% of their offspring are ventralized (the *dpp*^{H46}/*dpp*^{H46} embryos). The dorso-ventral ratios of luminescence were calculated using ventralized embryos only. Ventralized embryos were recognized by cuticle preparations, one day after imaging of the calcium patterns. The [put^{135}/TM3 [hb-Z]] line was kindly provided by Dr. Konrad Basler; 25% of their offspring are ventralized (the *put*^{135}/*put*^{135} embryos). The dorso-ventral ratios of luminescence were calculated using ventralized embryos only. Ventralized embryos were recognized by an X-gal staining (see above) about 2 h after the calcium measurements were ended (8 h of development). The ventralized *put*^{135}/*put*^{135} embryos do not show any staining, in contrast to the other genotypes which stain dark blue in the anterior half of the embryo.

RESULTS

Calcium Patterns in Wild-Type Embryos

Patterns of free cytosolic calcium were first imaged on an imaging photon detector after injection of the chemiluminescent calcium indicator *h*-aequorin into the Drosophila embryo. Calcium imaging with luminescence allows for long continuous recording without affecting development. Thus, the imaged embryos hatched as normal larve after 30 h of development. We investigated the patterns of calcium during the first 6 h of development and found striking gradients along the dorsoventral axis (Fig. 1). During early development (0–2.5 h), calcium concentrations were elevated in the ventral region of the embryo and oscillate along with the cell cycle (Fig. 1G). Early Drosophila development is characterized by nuclear division without cell division, indicating that these calcium oscillations are associated with the embryo's nuclear cycle. The lowest levels of calcium were observed at the end of stage 4 (2.5 h). These low calcium concentrations represent the "resting level" of calcium and averaged 72 nM (n = 18, SE = 6). Cell formation (stage 5) lasts for about an hour and calcium levels increase during this time. This calcium increase is most pronounced at the dorsal region, thus creating a stage 5 calcium gradient with high calcium dorsally. The calcium concentrations in the dorsal region averaged 107 nM (n = 18, SE = 10). The calcium gradient remains visible until the end of stage 6 (3 h 35 min). Calcium levels increase further in late embryonic development. These calcium elevations seem to be associated with gross morphological changes such as germ band extension and stomodeal invagination. Calcium levels reach a maximum of 137 nM (n = 18, SE = 11) during germ band extension (4 h 15 min). At 5.5 h, calcium gradients reverse for a second time to give high calcium concentrations ventrally. Thus, a total of three calcium gradients was observed along the dorsoventral axis during the first 6 h of development. We focused our investigation on the stage 5 gradient, which is the most pronounced.

To confirm the existence of a stage 5 calcium gradient, we imaged calcium using ratiometric confocal microscopy. Embryos were injected with a mixture of calcium green dextran and Texas red dextran. The ratio between these two is a measure of the calcium concentration. Again, we observed a late stage 5 calcium gradient with high calcium in the dorsal region (Fig. 2). This gradient was most pronounced at 3.5 h of development, which is somewhat later than expected on basis of the luminescent measurements. Possibly, the delay is

FIG. 1. Calcium patterns imaged in wild-type embryos during the first 6 h of development. Calcium was measured on an imaging photon detector after injection of the luminescent calcium indicator *h*-aequorin. (A–C) Bright-field images of an embryo during late-stage 4, late-stage 5, and mid-stage 7. Embryos are oriented dorsal up, anterior to the left. (D–F) Corresponding photon images. Luminescence was accumulated continuously, with 15-min counts centered over each time point, and color-coded using a spectrum from blue (2 photons/pixel) to red (12 photons/pixel). Note the calcium gradient during late-stage 5, calcium is higher dorsally than it is ventrally. (G) Calcium patterns were analyzed in more detail by plotting graphs of the dorsal region (in black) versus the ventral region (dashed, in red). The cytosolic free calcium concentration, [Ca^{2+}], was calculated from the level of luminescence, which is expressed in milliphotons/pixel second (mp/ps). Stage 5 is outlined by two dotted lines. (H) The dorsal/ventral (D/V) ratio was averaged (n = 18). The error bars indicate the standard error. The asterisks indicate a significant difference from a uniform calcium distribution (t test, $P < 0.01$).

FIG. 2. Ratiometric calcium imaging with confocal laser scanning microscopy confirms the existence of a late-stage 5 calcium gradient. (A) Image of a late-stage 5 embryo injected with a mixture of calcium green dextran (shown in green) and Texas red dextran (shown in red). The inner-embryonic region containing the yolk is nearly devoid of dye. (B) The calcium green/Texas red ratio was color-coded using a spectrum from blue (low calcium) to red (high calcium). On average, the dorsal region has a 9% higher ratio than the ventral region (n = 19, SE = 1.0%). This dorsal-ventral difference is significant (t test, $P < 0.001$). The "i" indicates a high calcium region associated with the injection wound. (C) A late-stage 5 embryo at high magnification. A high concentration of free calcium was measured in the dorsal nuclei. Embryos are positioned dorsal up, anterior to the left, scale bars are 50 μm.

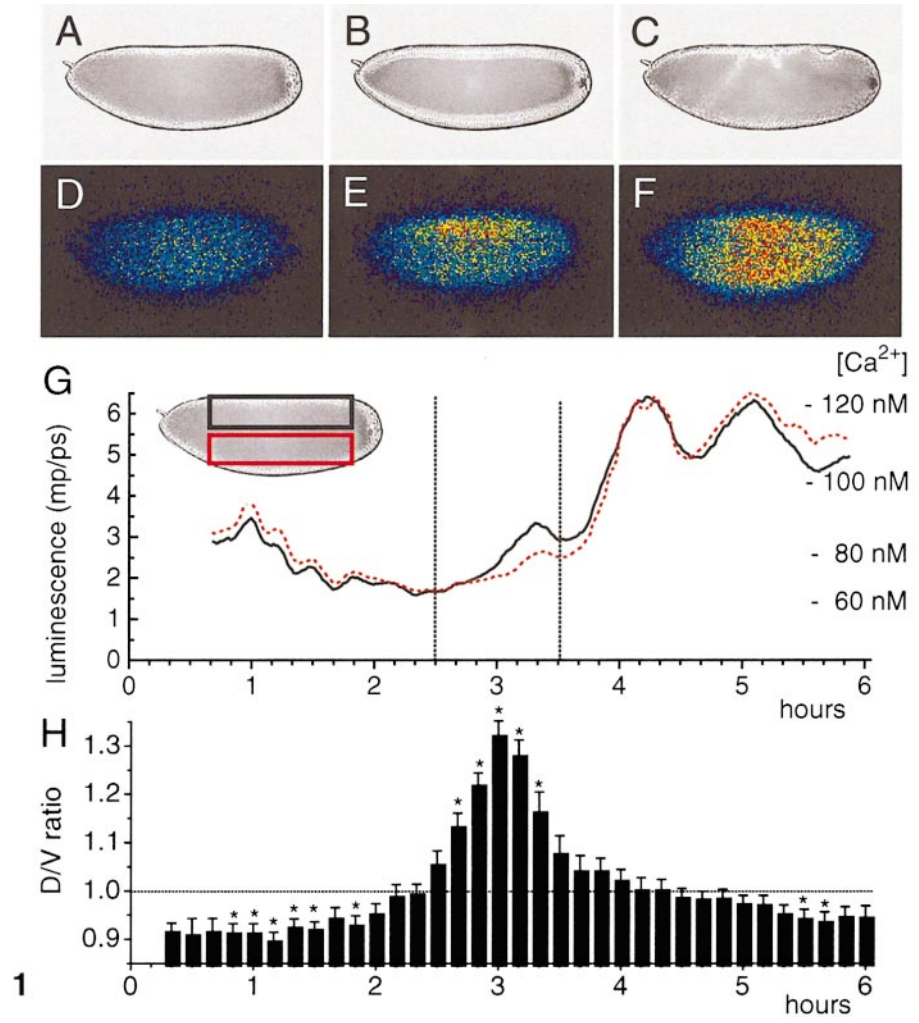

1

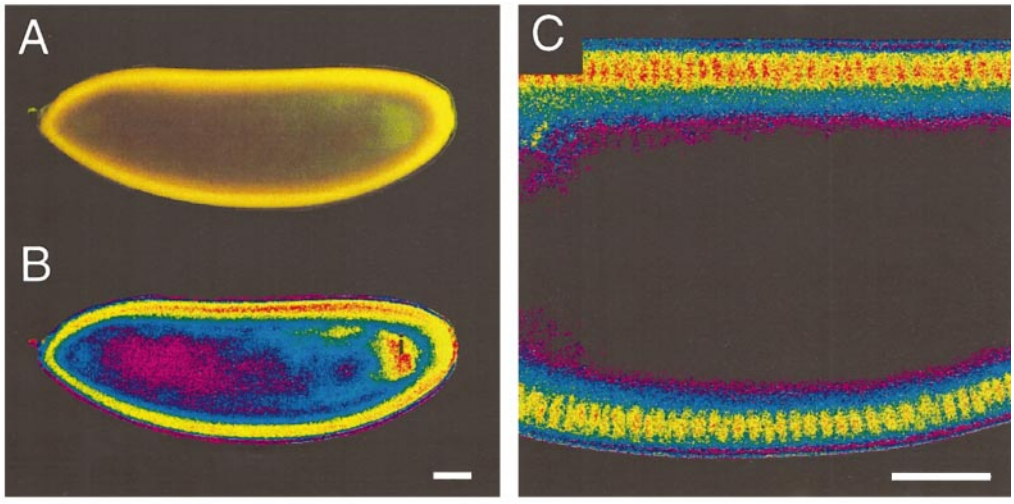

2

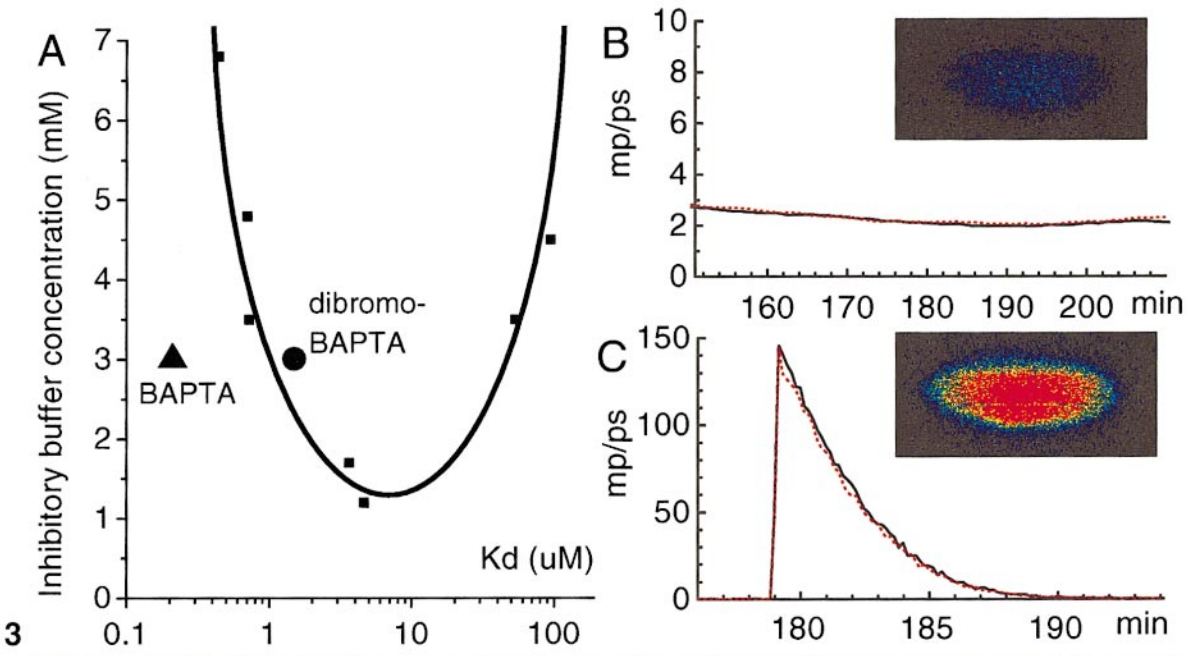

3

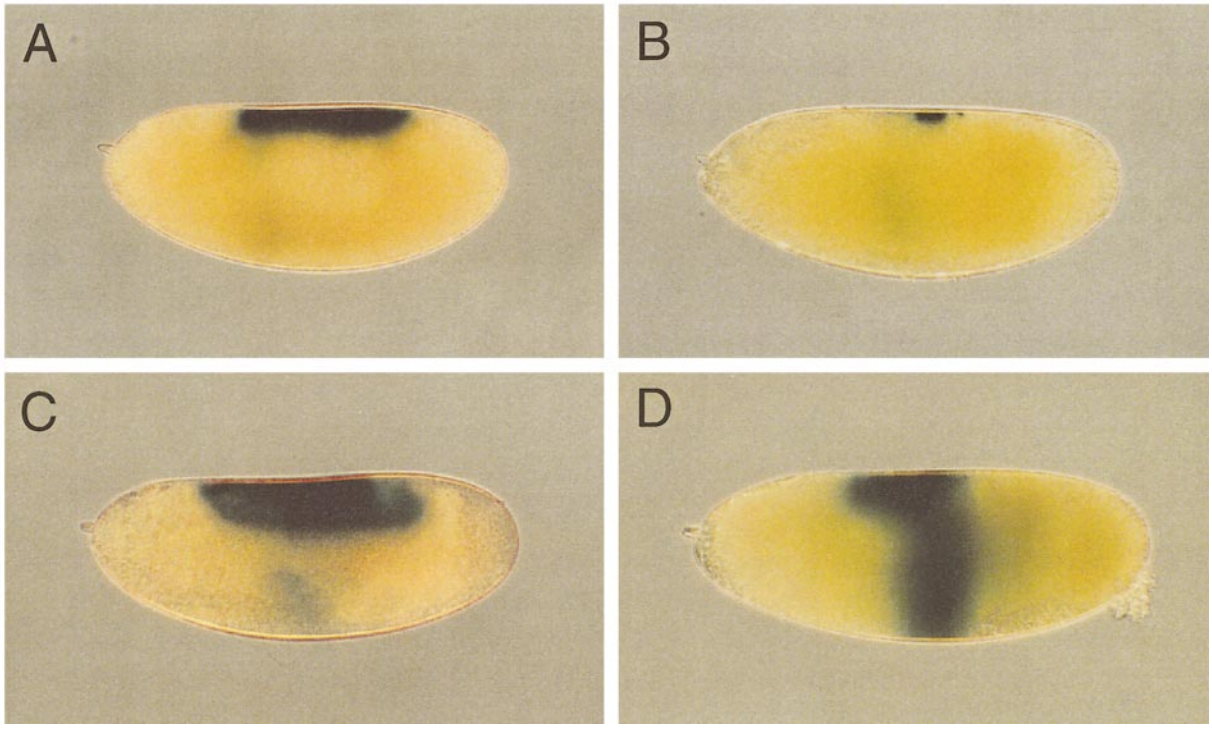

4

FIG. 3. Calcium patterns were manipulated by injection of BAPTA-type buffers. (A) The concentrations of straight BAPTA (triangle) and dibromo-BAPTA (circle) were compared to the concentrations of various BAPTAs that were needed to inhibit tip growth of the fucoid egg (squares); modified from Speksnijder *et al.* (1989). The inhibitory buffer concentration is strongly dependent on the K_d of the BAPTA. Note that dibromo-BAPTA falls within the inhibitory range, while straight BAPTA does not. (B) Injection of dibromo-$BAPTA_{50}$ at a final concentration of 3 mM inhibits the dorsal-ventral calcium gradient during stage 5 (150–210 min). The calcium patterns were imaged on the imaging photon detector. The average dorsal/ventral ratio during late-stage 5 is 0.98 (n = 13, SE = 0.02). The photon image shows a representative embryo in which calcium concentrations are uniformly low. (C) Injection of dibromo-$BAPTA_{2000}$ at a final concentration of 3 mM gives highly elevated calcium levels which gradually decreases in time. The $t_{1/2}$ is 2.5 min (n = 8, SE = 0.4), and elevated calcium concentrations can be observed for up to 20 min. The corresponding photon image shows a representative embryo in which calcium

caused by the buffering capacity of the fluorescent indicator, which is used at about a 10-fold higher concentration than the luminescent indicator. The dorsal/ventral ratio at 3.5 h averaged 1.09 ($n = 19$, SE = 0.01) and is significantly different from a uniform calcium distribution (*t* test, $P < 0.001$). The fluorescent ratios are smaller than the luminescent ratios. This difference in ratios can be explained by the properties of the indicators used. For aequorin luminescence is proportional to the 2.5 (Allen *et al.*, 1977) or to the 2.1 (Shimomura *et al.*, 1996) power of the calcium concentration and thus provides images with high contrast, while calcium green fluorescence varies no more than the first power of calcium. Moreover, fluorescent contrast (unlike luminescent contrast) is dimmed by autofluorescence. Even though calcium green gives little contrast, the confocal microscope is capable of generating images with excellent spatial detail. The most striking subcellular localization was the high level of calcium in the dorsal nuclei (Fig. 2C). It may be that this high nuclear calcium is real. However, calcium imaging with confocal microscopy can, in some cases, overestimate nuclear amplitudes (reviewed by Stricker and Whitaker, 1999). In any case, the dorsoventral difference in calcium concentrations was unmistakable in the cytosol as well as the nuclei. So one can be confident that stage 5 calcium is higher in the dorsal cytosol than in the ventral one.

Manipulation of the Dorsal Calcium Zone Affects Specification of the Dorsal Region

Injected BAPTA-type calcium buffers are known to permanently suppress calcium-dependent development by repeatedly carrying calcium from a source (such as a leaky region of the plasma membrane) to a calcium sink (such as the subsurface ER) into which they release this calcium. Such "shuttle buffers" thereby suppress the development of high calcium zones (Speksnijder *et al.*, 1989). Speksnijder *et al.* showed that the minimal buffer concentration required for suppression of development strongly depends on the dissociation constant or K_d of the BAPTA buffer. The resultant data fit a U-shaped curve that is reproduced in Fig. 3A. The optimal buffer K_d at the bottom of the curve corresponds to the average, natural calcium concentration in the effective high calcium zone. Stronger buffers with lower K_d's are less effective because they fail to release calcium near the sink, while weaker ones fail to bind it near the source.

With this in mind, we injected stage 5 embryos with straight BAPTA as well as dibromo-BAPTA, which have a K_d of 0.21 and 1.5 μM, respectively, at physiological salt concentrations (Pethig *et al.*, 1989). A remarkable quantitative correspondence with the shuttle buffer curve was found (Fig. 3A). The stage 5 dorsal calcium zone was completely suppressed by injection of dibromo-BAPTA at a final concentration of 3 mM (Fig. 3B), one which is expected to fully suppress micromolar high calcium zones. Dibromo-BAPTA reduced the dorsal/ventral ratio from a peak level of 1.32 (Fig. 1) down to 0.98 ($n = 13$, SE = 0.02). The same 3 mM concentration of straight BAPTA, which would be theoretically expected to only partially suppress a micromolar calcium zone, in fact partially reduced the dorsal/ventral ratio from 1.32 to 1.11 ($n = 7$, SE = 0.04). The calcium chelator EGTA was the least effective in suppressing the stage 5 calcium gradient, which fits well with the predicted failure to release calcium near the sink. The stage 5 dorsal/ventral ratio averaged 1.19 ($n = 6$, SE = 0.04) in embryos injected with EGTA at the same 3 mM final concentration. To elevate calcium concentrations during stage 5, we added calcium to the dibromo-BAPTA buffer to set the free calcium concentration at 2 μM. Upon injection, this buffer gives a large uniform calcium pulse which lasts for up to 20 min (Fig. 3C). These results indicate that the stage 5 calcium gradient can be effectively manipulated via direct and specific mechanisms.

To determine if BAPTA injection affects specification of the amnioserosa, the dorsal-most region of the embryo, we used a Drosophila line in which the amnioserosa element of *Kruppel* upstream region drives the expression of *lacZ* (Jacob *et al.*, 1991; Ferguson and Anderson, 1992a). The *Kr-lacZ* construct is exclusively expressed in the amnioserosa cells of stage 14 embryos (Fig. 4). As Fig. 4 shows, injection of dibromo-BAPTA during stage 5 strongly inhibited *Kr-lacZ* expression. This immediately indicated that the dorsal calcium zone is needed for the development of dorsal-specific gene expression. We also observed that *Kr-lacZ* expression was fully restored or "rescued" by raising the injectate's calcium to the micromolar level (Fig. 4C). This rescue further confirmed that the observed inhibition was a direct effect of suppressing the dorsal calcium zone. These calcium-rescued embryos showed the ectopic *Kr-lacZ* expression in 17 out of the 135 embryos (Fig. 4D). So high stage 5 calcium may prove to be sufficient as well as necessary for dorsal-specific gene expression.

concentrations are uniformly high. The graphs show luminescence of the dorsal region (in black) versus the ventral region (dashed, in red). Photon images are 15-min exposures, color-coded from blue (2 photons/pixel) to red (12 photons/pixel). The lowercase numbers in the BAPTA buffers indicate the free calcium concentration (in nM).

FIG. 4. Manipulation of stage 5 calcium gradient affects specification of the amnioserosa, the most dorsal region of the embryo. (A) Embryos from a *Kr-lacZ* line express β-galactosidase in the amnioserosa. (B) *Kr-lacZ* expression was absent or strongly inhibited after injecting dibromo-BAPTA$_{50}$ at a final concentration of 3 mM during mid-stage 5. (C) *Kr-lacZ* expression was rescued by adding calcium to the injectate; i.e., most embryos stained positive when injecting dibromo-BAPTA$_{2000}$ at a final concentration of 3 mM. (D) Dibromo-BAPTA$_{2000}$ injection induced ectopic *Kr-lacZ* expression in 13% of the embryos ($n = 135$).

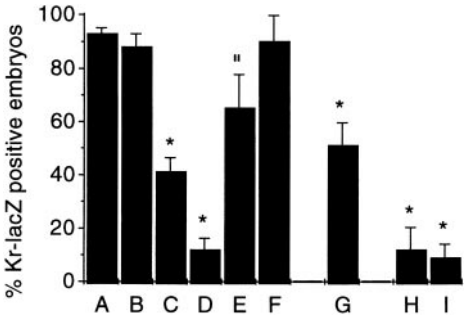

FIG. 5. The inhibition of *Kr-lacZ* expression was quantified. Various BAPTAs were injected during stage 5 and the percentage of embryos with positive *Kr-lacZ* expression was determined. (A) Control embryos, uninjected. Positive staining was observed in 93% of the embryos. To determine which concentration of dibromo-BAPTA is required for an inhibition of *Kr-lacZ* expression, we injected dibromo-BAPTA$_{50}$ at a final concentration of 0.75 mM (B), 1.5 mM (C), and 3 mM (D). To confirm that the inhibition of *Kr-lacZ* expression is a calcium effect, we injected 3 mM dibromo-BAPTA$_{2000}$ in which the free calcium concentration is set at 2 μM (E). The specificity of dibromo-BAPTA was determined by injection of straight K_4-BAPTA$_{50}$ at a 3 mM final concentration (F). To determine if the inhibition of *Kr-lacZ* can also be observed in morphologically normal embryos, we injected dibromo-BAPTA$_{50}$ at a 1.5 mM final concentration and determined the percentage of positives in stage 14 embryos only (G). To determine the stage specificity of the BAPTA injections, we injected stage 4 embryos with dibromo-BAPTA$_{50}$ (H) and dibromo-BAPTA$_{2000}$ (I) at a 3 mM final concentration. (*) indicates a significant difference as compared to column A. (") indicates a significant difference as compared to column D (t test, $P < 0.01$). Embryos were considered "positive" when at least half of the amnioserosa was stained. The lowercase numbers in BAPTA$_{50}$ and BAPTA$_{2000}$ indicate the free calcium concentration in these buffers (in nM). The error bars indicate the standard error. The number of experiments are 11, 5, 10, 9, 7, 3, 9, 7, and 4 and the corresponding number of embryos are 98, 45, 92, 93, 96, 16, 79, 57, and 44 for group A–I, respectively.

We then quantified *Kr-lacZ* inhibition by various buffer injections (Fig. 5). Control embryos, which were uninjected, expressed *Kr-lacZ* in 93% of the cases. Such expression is not significantly affected by injections which yield 0.75 mM dibromo-BAPTA. However, higher levels of dibromo-BAPTA do inhibit it. Injection of dibromo-BAPTA at a final concentration of 1.5 mM reduces *Kr-lacZ* expression to 41%. Injection of dibromo-BAPTA at a 3 mM final concentration, which grossly suppresses the dorsal zone, strongly inhibits *Kr-lacZ* expression. Only 12% of the embryos showed *Kr-lacZ* staining after such buffer injection in mid-stage 5. To confirm that *Kr-lacZ* inhibition results from calcium zone suppression, we injected a dibromo-BAPTA buffer during stage 5 in which the free calcium concentration was set at 2 μM. Such injection yields a large calcium pulse and proves to rescue most of the embryos. Thus 65% of these embryos express *Kr-lacZ* as compared to only 12% of those injected with dibromo-BAPTA without added calcium. Moreover, the straight BAPTA injections that ineffectively suppressed formation of a dorsal calcium zone were likewise ineffective in inhibiting *Kr-lacZ* expression; for 90% of the embryos showed *Kr-lacZ* staining after such injection.

Embryos injected with dibromo-BAPTA at a final concentration of 3 mM showed severe developmental abnormalities. The head fold and dorsal folds were mostly reduced or missing. In some cases, a head fold was formed which was symmetric along the dorsal-ventral axis. Cuticles were not formed in most of the embryos. Embryos that did form cuticles showed a reduced number of denticle belts, which were localized at their normal ventral position and did not seem to be extended or reduced along the dorsoventral axis. Mouth parts included normal mouth hooks, H-pieces, and ventral arms. However, the dorsal bridge and dorsal arms are often absent. This latter defect indicates a mild ventralization of the embryo (Wharton *et al.*, 1993). The lack of cuticle formation in the majority of the embryos may be expected, since calcium is a widely used messenger which probably affects many aspects of development. On the other hand, the signs of ventralization further support the concept that a high calcium zone is needed for dorsal development. We then investigated whether an inhibition of *Kr-lacZ* expression can be observed in embryos which develop normally according to morphological criteria. To this end, we selected those embryos which developed to a morphologically normal stage 14 after injection of dibromo-BAPTA at a 1.5 mM final concentration (60% of the injected embryos, $n = 79$). We found that the expression of *Kr-lacZ* was significantly inhibited in these morphologically normal stage 14 embryos; i.e., only half (49%) of the stage 14 embryos expressed *Kr-lacZ* (Fig. 5G). This experiment indicates that low concentrations of dibromo-BAPTA can inhibit specification of the amnioserosa without affecting the overall morphology of the stage 14 embryo.

Finally, to determine when *Kr-lacZ* inhibition occurs, we injected dibromo-BAPTA at a final concentration of 3 mM during late stage 4 rather than stage 5 (Fig. 5H). *Kr-lacZ* expression was strongly inhibited by this early injection, presumably because the injected buffer is still in the cytosol during stage 5. As we reported above, addition of calcium to this buffer gives a calcium pulse for 10–20 min (Fig. 3C) and rescues *Kr-lacZ* expression when it is injected during stage 5 (Fig. 5E). In contrast, *Kr-lacZ* expression was not rescued by injection of this same high calcium buffer during stage 4 (Fig. 5I). This experiment indicates that the calcium elevation must occur during stage 5 to induce *Kr-lacZ* expression.

Formation of the Stage 5 Calcium Gradient Is Downstream of dl

Calcium patterns were imaged in various mutants to determine at what point the calcium gradients are formed with respect to the signaling pathways which control pattern formation along the dorsal-ventral axis. We examined the mutants *pipe*, *Toll*, *dl*, *dpp*, and *punt* (Fig. 6). The Pipe, Toll, and Dl proteins play a role in induction of the ventral

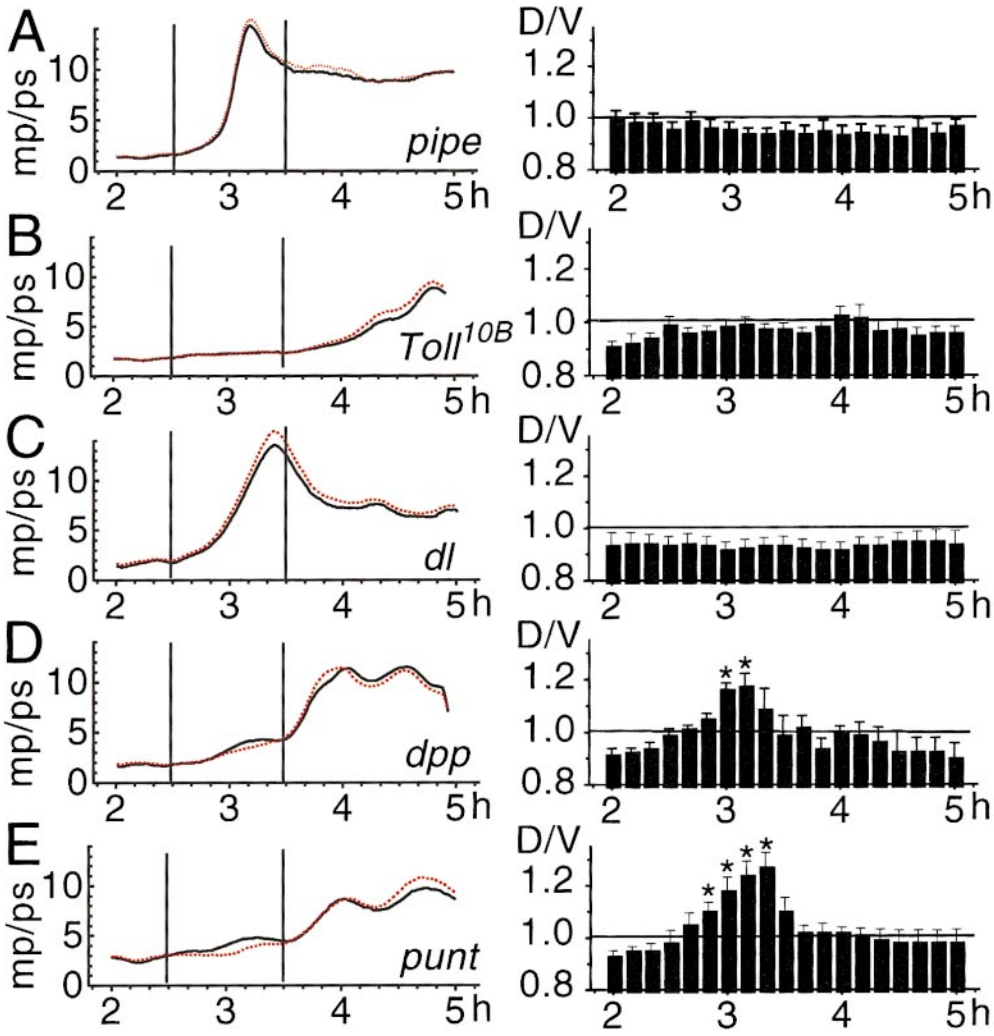

FIG. 6. Calcium patterns in mutant embryos. The left panels show the luminescence of individual mutant embryos from 2 to 5 h of development, in which the dorsal region (in black) and ventral region (dashed, in red) are compared. The right panels show the averaged dorsal/ventral (D/V) ratio during the same time period. (A) The dorsalized *pipe* mutant shows a strong calcium increase during stage 5 ($2\frac{1}{2}$–$3\frac{1}{2}$ h). High calcium levels are generated both dorsally and ventrally, thus eliminating the stage 5 calcium gradient ($n = 8$). (B) The ventralized *Toll*^{10B} mutant does not generate the typical stage 5 calcium increase at the dorsal region. Calcium levels remain low both ventrally and dorsally, thus eliminating the stage 5 calcium gradient ($n = 6$). (C) The dorsalized *dl* mutant has a calcium pattern similar to the *pipe* mutant, i.e., high calcium is generated both dorsally and ventrally, thus eliminating the stage 5 calcium gradient ($n = 6$). In fact, calcium levels are significantly higher ventrally than they are dorsally (significant differences were only indicated by asterisks when ratios are larger than 1.0). (D) The ventralized *dpp*^{H46} mutant generates calcium patterns indistinguishable from wild-type calcium patterns. It has a normal calcium elevation at the dorsal region of the embryo, thus creating a normal stage 5 calcium gradient ($n = 4$). (E) The ventralized *punt* mutant generates calcium patterns that are, again, indistinguishable from wild-type calcium patterns ($n = 5$). The increased D/V ratio during late stage 5 is significant in both the *dpp* and *punt* mutant (the asterisks indicate a significant difference from a uniform distribution, *t* test, $P < 0.05$). The altered calcium patterns in the first three mutants and the unaltered calcium patterns in the last two mutants suggest that the stage 5 calcium gradient is downstream of *pipe*, *Toll*, and *dl*, and upstream or independent of *dpp* and *punt*.

region, while the Dpp and Punt proteins play a role in induction of the dorsal region (see, e.g., Morisato and Anderson, 1995). The dorsalized *pipe*$^{-}$ embryos show highly elevated levels of calcium during stage 5 in the dorsal as well as the ventral region. The stage 5 calcium gradient is lost in these embryos (Fig. 6A). Pipe is a key regulator of dorsoventral specification during oogenesis (Sen *et al.*, 1998). The formation of the stage 5 calcium gradient is thus far downstream of this event. Calcium patterns were subsequently imaged in the *Toll*^{10B} mutant.

Toll^{10B} embryos are ventralized due to the overactive plasma membrane receptor Toll (Anderson *et al.*, 1985). These embryos did not show the typical dorsal calcium elevation during stage 5 and the stage 5 calcium gradient was lost (Fig. 6B). This indicates that the stage 5 calcium gradient is formed downstream of *Toll*. The dorsalized *dl*$^{-}$ embryos show highly elevated levels of calcium during stage 5 in the dorsal as well as the ventral region. The stage 5 calcium gradient is thus lost in these embryos (Fig. 6C). This shows that the formation of the calcium gradient is downstream of *dl*.

We then studied mutants with defects in the Dpp signaling pathway. First, we imaged calcium patterns in the *dpp* mutant. This mutant is ventralized due to defects in the ligand that normally induces the dorsal region of the embryo. The calcium patterns of the *dpp* mutant are indistinguishable from wild-type calcium patterns. We observed a normal calcium elevation at the dorsal region, creating a normal stage 5 calcium gradient (Fig. 6D). Similar results were obtained in the *punt* mutant. This mutant has defective type II Dpp-receptors (Ruberte *et al.*, 1995; Letsou *et al.*, 1995). Again, we observed a normal calcium elevation at the dorsal region, creating a normal stage 5 calcium gradient (Fig. 6E). The calcium patterns in the latter two mutants show that the formation of the stage 5 calcium gradient is upstream or independent of the Dpp signaling pathway.

The analysis of calcium patterns in mutant embryos shows that the formation of the stage 5 calcium gradient is downstream of *dl* and suggests that the Dl protein plays a role in formation of this calcium gradient by inhibiting ventral calcium elevations. At present it is not clear by which mechanisms Dl inhibits calcium concentrations in the ventral region. Possibly, nuclear Dl affects transcription of genes coding for calcium channels or calcium pumps. This modulation of gene expression may be a direct effect of Dl, or may be mediated by other proteins such as Twist or Snail. It is not clear either which mechanisms are responsible for the observed calcium elevation in the dorsal region during stage 5. We speculate that this calcium increase may be caused by formation of the cleavage furrows which activate stretch-sensitive calcium channels. This would cause a general calcium increase during stage 5, which would subsequently be inhibited on the ventral side by the Dl protein.

DISCUSSION

A Gradient with High Calcium in the Ventral Region

During early development (stages 1–4), a calcium gradient was observed with high levels of calcium in the ventral region. This gradient precedes Toll activation by at least 1.5 h and is unaffected in each of the imaged mutants (data not shown). The unaltered calcium gradient in *pipe*$^{-}$ mutants suggests that the ventral calcium elevation is not a downstream component of the signaling pathways during mid-oogenesis, which are activated when the nucleus moves to the future dorsal region and *pipe* is expressed in the ventral follicle cells (Sen *et al.*, 1998). The early calcium gradient with ventral high calcium is still present when Toll signaling is activated during the syncytial blastoderm stage. The Toll signaling pathway is known to induce a translocation of the Dl protein into the nucleus via several identified steps (Anderson, 1998). Studies in Drosophila cell lines suggest that calcium may affect one of these steps. It was shown that high concentrations of calcium can induce a rapid translocation of the Dl protein into the nucleus by destabilizing the anchor protein Cactus (Kubota *et al.*, 1993; Kubota and Gay, 1995). It is unlikely that the modest calcium gradient in the embryo can induce the translocation of the Dl protein by itself (if this were true *Toll*$^{-}$ embryos would develop normally). However, the observed calcium gradient might play a role during the syncytial blastoderm stage by enhancing the gradient of nuclear localized Dl protein. Elevated ventral calcium during stage 4 may thus contribute to specification of the ventral embryonic region. As discussed below, calcium plays an opposite role during stage 5.

A Gradient with High Calcium in the Dorsal Region

During stage 5 a reversed calcium gradient was observed. Thus, high calcium was generated in the dorsal region of the embryo. The timing and localization of this calcium elevation suggest a close correlation with the Dpp signaling pathway, which is activated in the dorsal region during cell formation and gastrulation (stages 5 and 6). The timing of Dpp signaling must be inferred from the activation of target genes, since Dpp forms an activity gradient which cannot be visualized directly (Wharton *et al.*, 1993). The earliest known effect of Dpp signaling is the transcriptional regulation of *zen* (Morisato and Anderson, 1995). Expression of *zen* is initially under maternal control. During stage 5 and 6, *zen* expression becomes gradually confined to the presumptive amnioserosa cells. Transcription of *zen* at this later stage requires zygotic *dpp* (Ray *et al.*, 1991). Thus the timing of Dpp action corresponds well to the appearance of the dorsal calcium zone, which is first seen at the beginning of stage 5 and lasts through stage 6. Moreover, by suppressing or relocating the dorsal calcium zone we showed that calcium plays an active role in specification of the dorsal most region. Suppression of dorsal calcium inhibited *Kr-lacZ* expression in the amnioserosa, while induction of an ectopic calcium zone could induce ectopic *Kr-lacZ* expression.

These results led us to believe that calcium had to be a second messenger in the Dpp signal transduction pathway. However, analysis of the mutants proved us wrong. As expected, the stage 5 calcium gradient was altered in *pipe*, *Toll*, and *dl* mutants. However, completely normal calcium

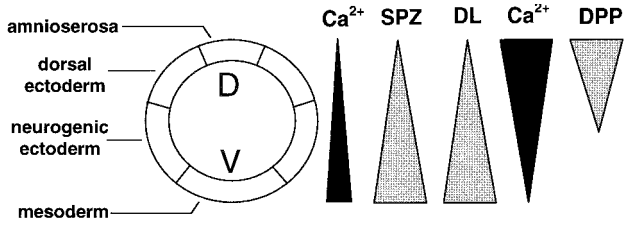

FIG. 7. Model showing subsequent gradients along the dorsoventral axis. The position of the calcium gradients with respect to various protein gradients was determined by mutant analysis. SPZ indicates the gradient of activated Spatzle in the perivitelline space, DL indicates the gradient of Dorsal protein localized in the syncytial nuclei, and DPP indicates the Dpp-activity gradient in the perivitelline space.

patterns were observed in *dpp* and *punt* mutants. Thus formation of the dorsal calcium zone does not require *dpp*. What model can explain these results? Perhaps the most straightforward model is a linear one, in which calcium acts as one of the steps in the series of events that determines pattern along the dorsal-ventral axis (Fig. 7). If correct, the dorsal calcium zone would act between *dl* and *dpp*. This may seem as an unlikely mechanism since it is generally believed that the Dl protein binds directly to the *dpp* promoter. On the other hand, there are no high-affinity binding sites for the Dl protein on the *dpp* promoter (Huang *et al.*, 1993), raising the possibility that there could be an intermediate step. From our results it is clear that Dl does inhibit a ventral calcium elevation; i.e., high ventral calcium was observed in *dl* mutants. However, it is not clear yet if a high calcium zone does indeed activate *dpp* expression. The activation of gene expression by calcium is currently an area of intense interest and a wide variety of mechanisms have been suggested (see, e.g., Ginty, 1997; Hardingham *et al.*, 1998). Most likely, calcium would activate transcription via calmodulin, which is abundantly present throughout embryogenesis (Beckingham, 1995).

However, the obtained results do not need to be explained by a linear model. The dorsal calcium zone may, for instance, steepen the Dpp-activity gradient by stimulating secretion of Dpp (or Dpp activators). In this case, the Dl protein would inhibit both transcription and secretion of Dpp. Alternatively, calcium may enhance Dpp action by interacting with cytosolic messengers such as the *Smad* proteins Mad and Medea. Interestingly, it was recently shown that calmodulin binds to the N-terminal of such *Smad* proteins (Zimmerman *et al.*, 1998).

In conclusion, a calcium gradient with high calcium in the dorsal region is generated in the Drosophila embryo during stage 5. This calcium gradient plays a role in specification of the dorsal-most region. However, the target proteins remain to be identified.

ACKNOWLEDGMENTS

We thank Carl Hashimoto for his help and advice on this project and acknowledge valuable discussions with Mike Levine and Elaine Bearer. Konrad Basler kindly provided some of the fly stocks and the aequorins were kindly provided by Osamu Shimomura, Satoshi Inouye, and Yoshito Kishi.

REFERENCES

Allen, D. G., Blinks, J. R., and Prendergast, F. R. (1977). Aequorin luminescence: Relation of light emission to calcium concentration. *Science* **196,** 996–998.

Anderson, K. V., Jurgens, G., and Nusslein-Volhard, C. (1985). Establishment of dorsal-ventral polarity in the Drosophila embryo: Genetic studies on the role of the Toll gene product. *Cell* **42,** 779–789.

Anderson, K. V. (1998). Pinning down positional information: Dorsal-Ventral polarity in the Drosophila embryo. *Cell* **95,** 439–442.

Ashe, H. L., and Levine, M. (1999). Local inhibition and long-range enhancement of Dpp signal transduction by Sog. *Nature* **398,** 427–431.

Beckingham, K. (1995). Calcium regulation of Drosophila development. *Adv. Sec. Mess. Phosph. Res.* **30,** 359–394.

Belvin, M. P., and Anderson, K. V. (1996). A conserved signaling pathway: the Drosophila toll-dorsal pathway. *Annu. Rev. Cell Dev. Biol.* **12,** 393–416.

Créton, R., Kreiling, J. A., and Jaffe, L. F. (1999). Calcium imaging with chemiluminescence. *Microsc. Res. Tech.* **46,** 390–397.

Ferguson, E. L., and Anderson, K. V. (1992a). Decapentaplegic acts as a morphogen to organize dorsal-ventral pattern in the Drosophila embryo. *Cell* **71,** 451–461.

Ferguson, E. L., and Anderson, K. V. (1992b). Localized enhancement and repression of the activity of the TFG-β family member, decapentaplegic, is necessary for dorsal-ventral pattern formation in the Drosophila embryo. *Development* **114,** 583–597.

Ferguson, E. L. (1996). Conservation of dorsal-ventral patterning in arthropods and chordates. *Curr. Opin. Genet. Dev.* **6,** 424–431.

Ginty, D. D. (1997). Calcium regulation of gene expression: Isn't that spatial? *Neuron* **18,** 183–186.

Hardingham, G. E., Cruzalegui, F. H., Chawla, S., and Bading, H. (1998). Mechanisms controlling gene expression by nuclear calcium signals. *Cell Calcium* **23,** 131–134.

Holley, S. A., and Ferguson, E. L. (1997). Fish are like flies are like frogs: Conservation of dorsal-ventral patterning mechanisms. *Bioessays* **19,** 281–284.

Huang, J. D., Schwyter, D. H., Shirokawa, J. M., and Courey, A. J. (1993). The interplay between multiple enhancer and silencer elements defines the pattern of decapentaplegic expression. *Genes Dev.* **7,** 694–704.

Jacob, Y., Sather, S., Martin J. R., and Ollo, R. (1991). Analysis of Kruppel control elements reveals that localized expression results from the interaction of multiple subelements. *Proc. Natl. Acad, Sci. USA* **88,** 5912–5916.

Jaffe, L. F. (1986). Ventral activation process in insect oocytes. *Nature* **321,** 386.

Kubota, K., Keith, F. J., and Gay, N. J. (1993). Relocalization of Drosophila dorsal protein can be induced by a rise in cytoplasmic calcium concentration and the expression of constitutively active but not wild-type Toll receptors. *Biochem. J.* **296,** 497–503.

Kubota, K., and Gay, N. J. (1995). Calcium destablizes Drosophila cactus protein and dephosphorylates the dorsal transcription factor. *Biochem. Biophys. Res. Commun.* **214,** 1191–1196.

Letsou, A., Arora, K., Wrana, J. L., Simin, K., Twombly, V., Jamal, J., Staehling-Hampton, K., Hoffmann, F. M., Gelbart, W. M., Massague, J., and O'Connor, M. B. (1995). Drosophila Dpp signalling is mediated by the punt gene product: A dual ligand-binding type II receptor of the TGFb receptor family. *Cell* **80,** 899–908.

Marques, G., Musacchio, M., Shimell, M. J., Wunnenberg-Stapleton, K., Cho, K. W., and O'Connor, M. B. (1997). Production of a Dpp activity gradient in the early Drosophila embryo through the opposing actions of the SOG and TLD proteins. *Cell* **91,** 417–426.

Massagué, J., Attisano, L., and Wrana, J. L. (1994). The TGF-β family and its composite receptors. *Trends Cell Biol.* **4,** 172–178.

Massagué, J. (1998). TGF-beta signal transduction. *Annu Rev. Biochem.* **67,** 753–791.

Morisato, D., and Anderson, K. V. (1995). Signaling pathways that establish the dorsal-ventral pattern of the Drosophila embryo. *Annu. Rev. Genet.* **29,** 371–399.

Mullins, M. C. (1998). Holy tolloido: Tolloid cleaves SOG/Chordin to free DPP/BMPs. *Trends Genet.* **14,** 127–129.

Nelson, H. B., Heiman, R. G., Bolduc, C., Kovalick, G. E., Whitley, P., Stern, M., and Beckingham, K. (1997). Calmodulin point mutations affect Drosophila development and behavior. *Genetics* **147,** 1783–1798.

Padgett, R. W., St Johnston, D., and Gelbart, W. M. (1987). A transcript from a Drosophila pattern gene predicts a protein homologous to the transforming growth factor-β family. *Nature* **325,** 81–84.

Pethig, R., Kuhn, M., Payne, R., Adler E., Chen, T. H., and Jaffe, L. F. (1989). On the dissociation constants of BAPTA-type calcium buffers. *Cell Calcium* **10,** 491–498.

Raftery, L. A., and Sutherland, D. J. (1999). TGF-beta family signal transduction in Drosophila development: From Mad to Smads. *Dev. Biol.* **210,** 251–268.

Ray, R., Arora, K., Nusslein-Volhard, C., and Gelbart, W. M. (1991). The control of cell fate along the dorsal-ventral axis of the Drosophila embryo. *Development* **113,** 35–54.

Roth, S., Stein, D., and Nusslein-Volhard, C. (1989). A gradient of nuclear localization of the dorsal protein determines dorsoventral pattern in the Drosophila embryo. *Cell* **59,** 1189–1202.

Ruberte, E., Marty, T., Nellen, D., Affolter, M., and Basler, K. (1995). An absolute requirement for both the type II and type I receptors, punt and thick veins, for Dpp signalling in vivo. *Cell* **80,** 889–897.

Rushlow, C. A., Han, K., Manley, J. L., and Levine, M. (1989). The graded distribution of the dorsal morphogen is initiated by selective nuclear transport in Drosophila. *Cell* **59,** 1165–1177.

Sen, J., Goltz, J. S., Stevens, L., and Stein, D. (1998). Spatially restricted expression of pipe in the Drosophila egg chamber defines embryonic dorsal-ventral polarity. *Cell* **95,** 471–481.

Shimomura, O., and Inouye, S. (1996). Titration of recombinant aequorin with calcium chloride *Biochem. Biophys. Res. Commun.* **221,** 77–81.

Speksnijder, J. E., Miller, A. L., Weisenseel, M. H., Chen, T. H., and Jaffe, L. F. (1989). Calcium buffer injections block fucoid egg development by facilitating calcium diffusion. *Proc. Natl. Acad. Sci. USA* **86,** 6607–6611.

Steward, R. (1989). Relocalization of the dorsal protein from the cytoplasm to the nucleus correlates with its function. *Cell* **59,** 1179–1188.

Stricker, S. A., and Whitaker, M. (1999). Confocal laser scanning microscopy of calcium dynamics in living cells. *Microsc. Res. Tech.* **46,** 356–369.

Ten Dijke, P., Miyazono, K., and Heldin, C. H. (1996). Signaling via hetero-oligomeric complexes of type I and type II serine/threonine kinase receptors. *Curr. Opin. Cell Biol.* **8,** 139–145.

Wall, N. A., and Hogan, B. L. M. (1994). TGF-β related genes in development. *Curr. Opin. Gen. Dev.* **4,** 517–522.

Wharton, K. A., Ray, R. P., and Gelbart, W. M. (1993). An activity gradient of decapentaplegic is necessary for the specification of dorsal pattern elements in the Drosophila embryo. *Development* **117,** 807–822.

Wieschaus, E., and Nusslein-Volhard, C. (1986). Looking at embryos. In "Drosophila a Practical Approach" (D. B. Roberts, Ed), pp. 199–227. IRL press, Washington, DC.

Zimmerman, C. M., Kariapper, M. S., and Mathews, L. S. (1998). Smad proteins physically interact with calmodulin. *J. Biol. Chem.* **273,** 677–680.

Received August 23, 1999
Revised October 22, 1999
Accepted October 22, 1999